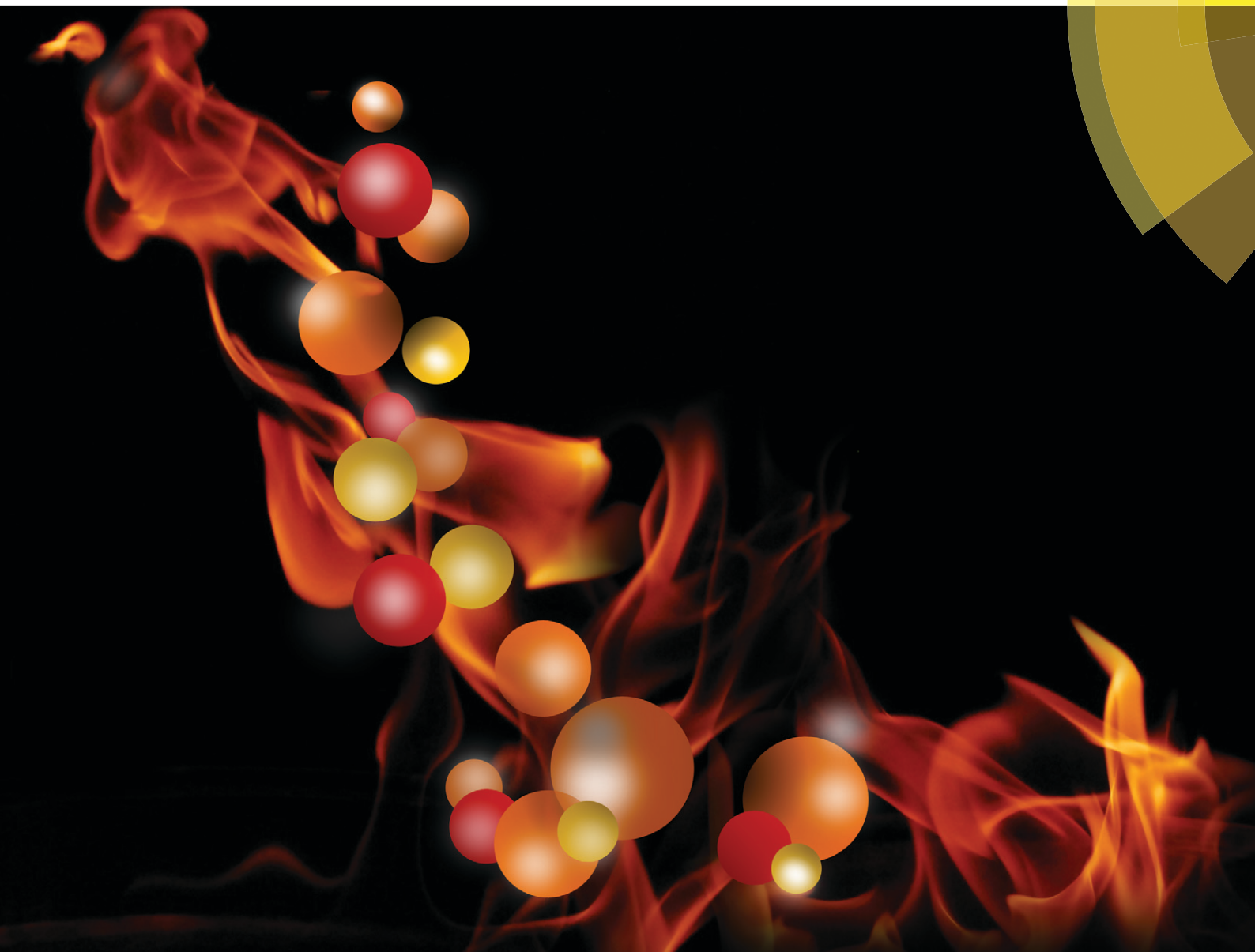# Environmental Science
Nano

ROYAL SOCIETY OF CHEMISTRY

PAPER
Linsey C. Marr *et al.*
Toxicity of particulate matter from incineration of nanowaste

Environmental Science Nano

PAPER

CrossMark
click for updates

Toxicity of particulate matter from incineration of nanowaste†

Eric P. Vejerano, Yanjun Ma, Amara L. Holder, Amy Pruden, Subbiah Elankumaran and Linsey C. Marr*

Disposal of some nanomaterial-containing waste by incineration and the subsequent formation of particulate matter (PM) along with hazardous combustion by-products are inevitable. The effect of nanomaterials on the toxicity of the PM is unknown. We assessed the oxidative potential (OP) and toxicity of PM resulting from the incineration of pure nanomaterials and of paper and plastic wastes containing Ag, NiO, TiO_2, ceria, C_{60}, Fe_2O_3, or CdSe/ZnS quantum dots (CdSe QD) at mass loadings ranging from 0.1 wt% to 10 wt%. We measured reactive oxygen species (ROS) using the dichlorofluorescein assay, and we also measured consumption of ascorbic acid, dithiothreitol (DTT), glutathione (GSH), or uric acid antioxidants from raw and solvent-extracted PM, denoted "cleaned PM". We determined cytotoxicity and genotoxicity of PM to A549 human lung epithelial cells with the WST-1 cell viability and histone immunofluorescence assays, respectively. In most cases, the presence of nanomaterials in the waste did not significantly affect the OP of PM; however, PM derived from waste containing Ag, TiO_2, and C_{60} had elevated ROS response in the GSH and DTT assays. The ratio of reduced to oxidized glutathione was significantly higher for cleaned PM compared to raw PM for almost all nanomaterials at almost all concentrations, indicating that combustion by-products adsorbed on raw PM play an important role in determining OP. The presence of nanomaterials did not significantly modify the cytotoxicity or genotoxicity of the PM. Different antioxidants used to assess OP had varying sensitivity towards organic compounds v. metals in PM. The presence of these seven nanomaterials at low concentrations in the waste stream is not expected to exacerbate the hazard posed by PM that is produced by incineration.

Nano impact

As more engineered nanomaterials are incorporated into consumer products, nanomaterials will inevitably enter the waste stream, and it is certain that some will be incinerated. The toxicity of nanomaterials stemming from the incineration on nanowaste is unknown. Incineration can modify the physicochemical properties of a nanomaterial and the emitted particulate matter and potentially alter their toxicity.

Introduction

New and novel applications of nanomaterials have driven rapid growth in nanoscience and nanotechnology. Disposal is inevitable, and some of the nanomaterials will be incinerated. Incineration produces large amounts of combustion by-products, including particulate matter (PM), also known as fly ash. Many modern incineration plants are equipped with air pollution control devices that capture PM and hazardous pollutants effectively, but some pollutants can circumvent air pollution control devices.[1] Additionally, open burning, which is still prevalent in some parts of the world for waste disposal, is a potential source of exposure to humans and animals. Many epidemiological studies have linked exposure to PM with various diseases ranging from asthma to cancer.[2-8]

Studies on the toxicity of nanoparticles and PM are abundant in the literature, but the toxicity of PM from incineration of waste containing nanomaterials has not been investigated, to our knowledge. We recently reported that because of the highly catalytic surface of some nanomaterials, their incineration can lead to the formation of elevated amounts of combustion by-products that can adsorb onto PM.[9] Some nanomaterials retain their physical and chemical properties during combustion,[10] while others are altered. The combination of these factors can potentially modify the toxicity of PM in combustion exhaust.

*Corresponding author, Civil and Environmental Engineering Department, Virginia Tech, 411 Durham Hall, Blacksburg, VA 24061, USA.
E-mail: lmarr@vt.edu; Fax: +1 (540) 231 7916; Tel: +1 (540) 231 6071
† Electronic supplementary information (ESI) available: TEM micrographs of PM, metal content in the waste. See DOI: 10.1039/c4en00182f

While the characteristics of PM that impart toxic effects are unknown, toxicity is generally attributed to the generation of reactive oxygen species (ROS):[11–14] hydrogen peroxide, superoxide, and the hydroxyl radical, the latter being the most damaging.[15–18] ROS are essential in cellular processes, chemical signal transduction, and immune function, and as a source of energy, but the overproduction of ROS causes oxidative stress: the body overreacts and triggers a stress response.[19–27] Biological systems can counter ROS *via* antioxidants such as endogenous glutathione, ascorbic acid, and uric acid, but elevated formation of ROS can make the defense system fail and can cause structural damage to cellular and molecular components.[28–30] For instance, 1.4 nm gold, 25 nm silver, and Fe_2O_3 nanoparticles generate ROS that cause cell damage and alter gene expression.[31–33] Nonmetallic nanomaterials such as fullerenes can also generate ROS.[34]

Some nanomaterials may also induce cytotoxic or genotoxic responses, including necrosis, apoptosis, or necroptosis. Cytotoxicity of nanomaterials proceeds *via* a number of different mechanisms and can be assessed using, for example, colorimetric methods to measure mitochondrial enzymatic activity and cell membrane integrity. Multi-walled carbon nanotubes in sufficient dose induce apoptosis in human lymphocytes,[35] gold nanoparticles can compromise cell membrane integrity,[36] and <10 nm silver nanoparticles exhibit toxicity to human lung cells.[37] Nanomaterials are predicted to induce genotoxicity *via* mechanisms such as gene mutations, clastogenic effects such as those exerted by ROS, and aneugenic mechanisms such as disruption of the spindle/mitotic apparatus.[38,39] Colloidal aqueous suspensions of fullerenes have been observed to exhibit genotoxic effects on some bacteria.[40] Silver nanoparticles can cause DNA damage *via* elevated ROS concentrations, with the damage being enhanced by the deposition of nanoparticles onto the DNA.[41]

We have employed an array of acellular and cell-based assays to investigate the OP, cytotoxicity, and genotoxicity of PM produced from incineration of waste containing nanomaterials. We examined metals/metal oxides, fullerenes, and quantum dots, selected to be representative of the major classes of nanomaterials in current use. Metals are of interest because some, such as iron, catalyze ROS formation,[14] which can produce pro-inflammatory effects.[42–44] Results can be used to inform risk assessments of nanotechnology and the development of policies to ensure the safe disposal of nanomaterials.

Results

We measured the OP of PM produced by the incineration of waste containing one of seven types of engineered nanomaterials: Ag, NiO, TiO_2, ceria, Fe_2O_3, C_{60}, or CdSe/ZnS quantum dots (CdSe QD). The PM was collected from the exhaust on filters and resuspended in ethanol. To separate the effects of organic compounds adsorbed to particles, we evaluated both raw PM (rPM) and cleaned PM (cPM), from which organic compounds had been removed by solvent extraction. In addition to three different loadings of the nanomaterial in the waste (0.1, 1, and 10 wt%), we also considered incineration of the pure nanomaterial without any other waste. Controls included rPM and cPM negative controls generated by incineration of waste with no added nanomaterials and a positive control of H_2O_2. We tested the PM for OP, cytotoxicity, and genotoxicity and defined differences between treatments to be significant at $p < 0.05$. We did not assess the toxicity of the pure nanomaterials in cellular systems because there is already abundant literature on this subject.

Hydrodynamic size of PM

The hydrodynamic size, defined as the diameter of a sphere that has similar diffusivity in solution as the particle, was larger for rPM than for cPM for most nanomaterials (Table 1). The removal of the shell of organic species by solvent extraction may have resulted in smaller size and reduced particle aggregation. For most of the rPM samples, the particle size was larger compared to the control. For most nanomaterials, differences in size between rPM and cPM for the same nanomaterial were statistically significant. Our prior work reports the effect of nanomaterials on the aerodynamic size of PM;[45]

Table 1 Hydrodynamic size of PM in phosphate buffered saline (PBS) with 0.1 wt% Tween-20

| Nanomaterial | Hydrodynamic size (nm) | | | | | |
| | 0.1 wt% | | 1 wt% | | 10 wt% | |
	rPM	cPM	rPM	cPM	rPM	cPM
Ag	540 ± 50^b	250 ± 1^a	400 ± 8^b	250 ± 10^a	390 ± 45^b	260 ± 20^a
NiO	290 ± 30	190 ± 10^a	320 ± 8^b	390 ± 40^b	250 ± 8	230 ± 4^a
TiO_2	330 ± 20^b	230 ± 7^a	280 ± 20	240 ± 50	300 ± 17	250 ± 6^a
Ceria	340 ± 6^b	210 ± 8^a	350 ± 25^b	230 ± 2^a	430 ± 13^b	200 ± 3^a
C_{60}	350 ± 3^b	300 ± 80^a	360 ± 7^b	250 ± 10^a	490 ± 14^b	220 ± 10^a
Fe_2O_3	300 ± 4^b	320 ± 70	290 ± 7	210 ± 1^a	361 ± 20^b	$180 \pm 1^{a,b}$
CdSe QD	300 ± 10^b	230 ± 10^a	330 ± 45	230 ± 3	380 ± 14^b	210 ± 10^a
None (control)	270 ± 3^c	230 ± 20^c				

^{a} Significantly different in size from rPM at $p < 0.05$. ^{b} Significantly different from corresponding control at $p < 0.05$ polydispersity index: rPM (0.315 ± 0.094), cPM (0.159 ± 0.047). ^{c} Measurements correspond to 0 wt% and are listed in this column for convenience.

the median size was unchanged at a loading of 0.1 wt% and was smaller than the control at a loading of 10 wt%.

ROS production in acellular assays

Fig. 1–5 show the results of various assays of ROS formation. In Fig. 1, 2, 3, and 5, higher y-axis values represent an increase in ROS formation, while in Fig. 4, lower y-axis values represent an increase in ROS formation. The solid gray bars represent the corresponding PM control and the positive control (H_2O_2). To determine if the PM induced oxidative stress, we used non-fluorescent dichlorodihydrofluorescein (DCFH) as a chemical marker, which is oxidized by ROS to fluorescent dichlorofluorescein (DCF). Fig. 1 shows that the change in fluorescence intensity for rPM and cPM ranged from ~40% to 50%. However, results for most samples were not significantly different compared to the unspiked control waste except for the pure CdSe QD nanoparticles. Pure C_{60} had significantly lower fluorescence intensity than did the cPM control. The differences in fluorescence intensity between rPM and cPM were not significant for a specific nanomaterial at a specific mass loading except for 10 wt% ceria, 0.1 wt% C_{60}, and 0.1 wt% and 10 wt% Fe_2O_3 (Table 2).

Antioxidants, such as ascorbic acid, act to scavenge ROS, and therefore their depletion can indicate the presence of ROS.[46] rPM and cPM consumed 40% to 70% of ascorbic acid (Fig. 2) for waste containing nanomaterials and lower amounts for certain pure nanomaterials. However, ascorbic acid consumption for most rPM and cPM samples was not

significantly different compared to the respective PM control except for rPM produced by 10 wt% CdSe QD. Ascorbic acid consumption was also significantly lower than the PM control for pure TiO_2, ceria, C_{60}, and CdSe QD nanoparticles. In most cases, the consumption of ascorbic acid in samples containing the same loading and type of nanomaterials was not significantly different between cPM and rPM except in a few cases as shown in Table 2. The positive control, H_2O_2, completely depleted ascorbic acid.

Similar to ascorbic acid, uric acid is an antioxidant that counteracts the effects of ROS, and hence loss of uric acid indicates formation of ROS. Consumption of uric acid was low, only ~1.5% to ~3.5% and not significantly different from that of the PM control, except for the pure CdSe QD nanoparticles (Fig. 3). For most samples, the levels of consumption were similar for rPM and cPM except for 0.1 wt% C_{60} and 10 wt% CdSe QD (Table 2). Even with H_2O_2, the consumption was less than 5%. Although the amount of antioxidant consumed was low compared to ascorbic acid, there was ROS consumption, and to a lesser extent, adsorption onto the particles. The low values were not attributable to variation due to instrument response and/or sample degradation. The relative standard deviation for triplicate measurements of three of the calibration standards during the analysis was less than 0.2%.

In biological systems, glutathione exists in both reduced form (GSH, 90–95% of the total glutathione) and oxidized form (GSSG). At high ROS concentration, more GSSG is produced; therefore, a decrease in the ratio of reduced to oxidized glutathione (GSH/GSSG) indicates greater OP. The
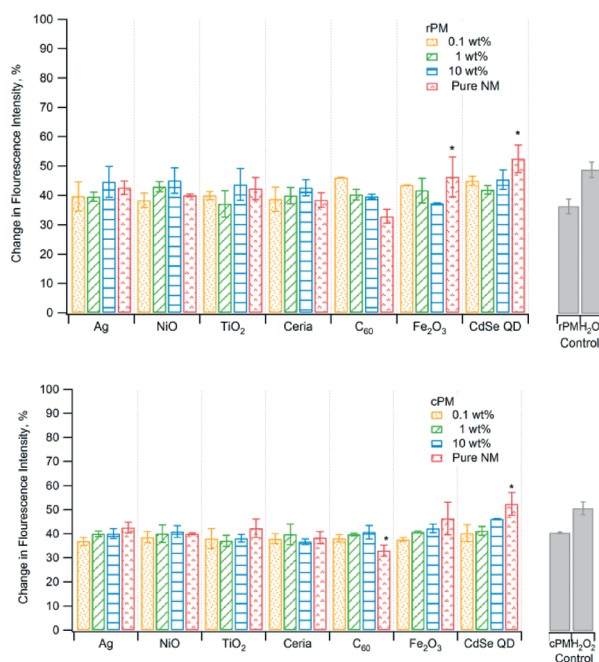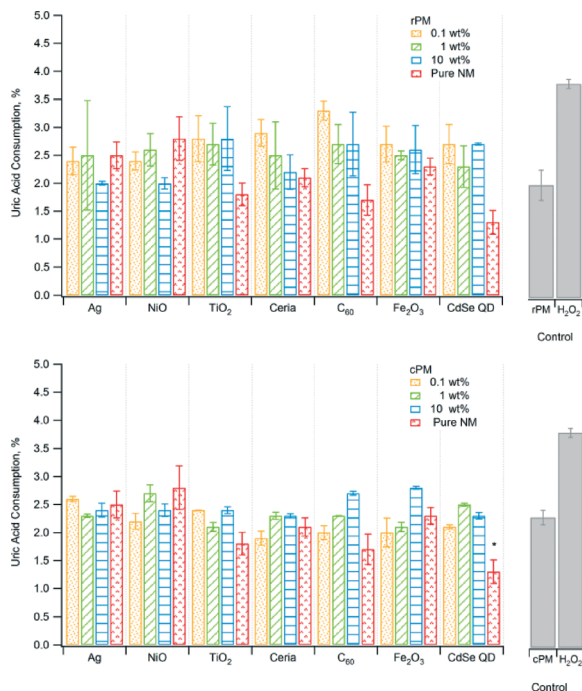

Fig. 1 Formation of DCF by raw PM (rPM) and cleaned PM (cPM). *Indicates significant difference relative to the corresponding unspiked rPM or cPM control at $p < 0.05$. The change in flourescence intensity was compared relative to the blank (ethanol). The PM concentration in suspension was 3.5 µg mL^{-1}.
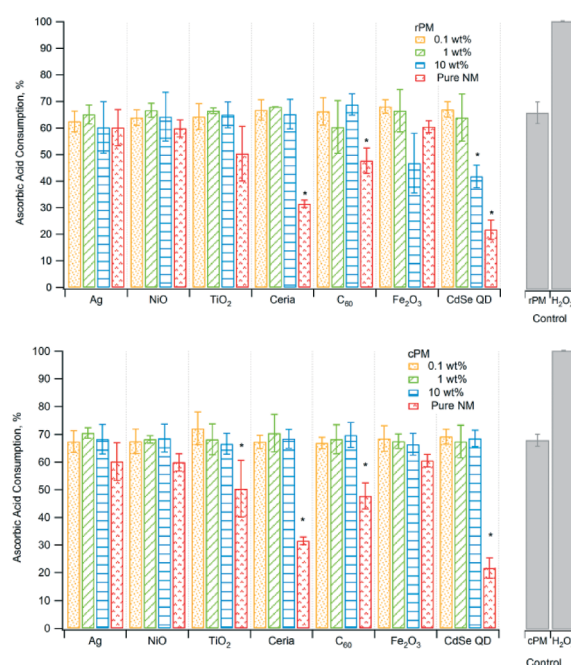
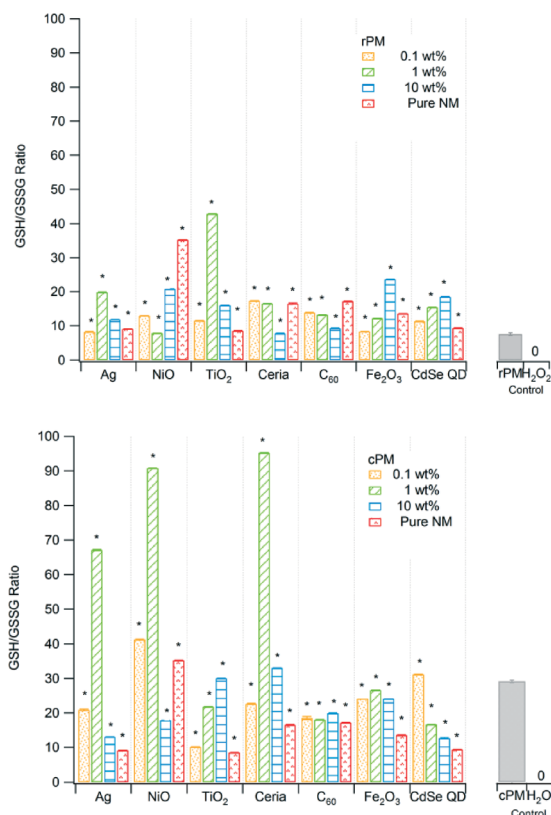
Fig. 2 Ascorbic acid consumption of raw PM (rPM) and cleaned PM (cPM). *Indicates significant difference relative to the corresponding unspiked rPM or cPM control at $p < 0.05$. The PM concentration in suspension was 3.5 µg mL^{-1}.
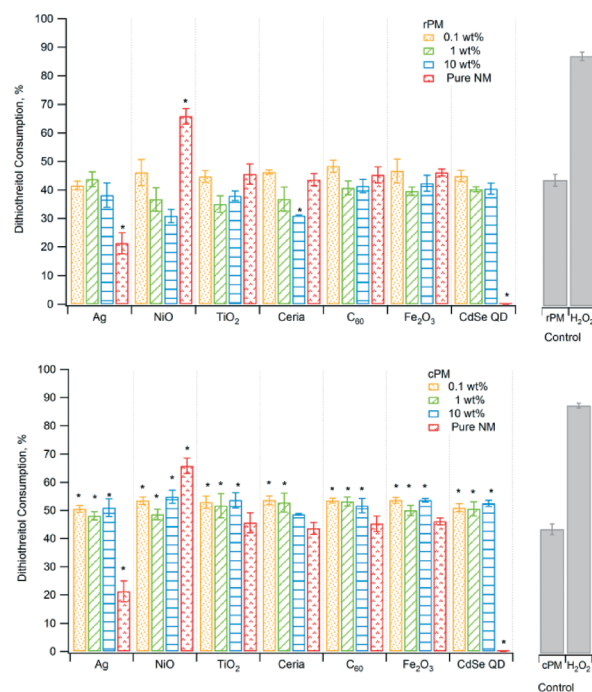
Fig. 3 Uric acid consumption of raw PM (rPM) and cleaned PM (cPM). *Indicates significant difference relative to the corresponding unspiked rPM or cPM control at $p < 0.05$. The PM concentration in suspension was 3.5 μg mL^{-1}.

Fig. 4 Ratio of reduced to oxidized glutathione (GSH/GSSG) for raw PM (rPM) and cleaned PM (cPM). A lower ratio indicates greater ROS formation. *Indicates significant difference relative to the corresponding unspiked rPM or cPM control at $p < 0.05$. The PM concentration in suspension was 3.5 μg mL^{-1}.

GSH/GSSG ratios for rPM ranged from ~10 to ~45 and from ~10 to ~100 for cPM (Fig. 4), and all combinations of type of nanomaterial and loading were significantly different from the PM control. The ratios of reduced to oxidized glutathione (GSH/GSSG) were significantly different between rPM and cPM for all nanomaterials at all concentrations (Table 2). Ratios for rPM were lower than for cPM except those containing 0.1 and 1 wt% TiO$_2$, 10 wt% NiO, and 10 wt% CdSe QD. The rPM control had higher OP (lower ratio) than did the samples with nanomaterials.

Dithiothreitol (DTT) is not present in biological systems but is highly sensitive to oxidation from components in PM that are redox-active, and hence DTT is used routinely in assessing OP of PM. Oxidation of DTT by ROS converts DTT to its disulfide form. Loss of DTT indicates OP. Consumption of DTT by the PM ranged from 30% to 55% (Fig. 5). DTT depletion was not significantly different compared to that in the PM control. Pure NiO nanoparticles consumed significantly more DTT than did the PM control, and pure CdSe QD and Ag consumed less. In fact, pure CdSe QD did not consume any measurable DTT. For cPM, DTT consumption for all samples, except pure TiO$_2$, 10 wt% ceria, pure ceria, pure C$_{60}$, and pure Fe$_2$O$_3$, was significantly different compared to the cPM control. For cPM, DTT consumption in all samples, except pure TiO$_2$, 10 wt% ceria, pure ceria, pure C$_{60}$, and pure Fe$_2$O$_3$, was significantly different compared to the cPM control. In addition, differences in DTT loss between rPM and cPM were significant for all nanomaterials at all concentrations (Table 2).

Fig. 5 DTT consumption of raw PM (rPM) and cleaned PM (cPM). *Indicates significant difference relative to the corresponding unspiked rPM or cPM control at $p < 0.05$. The PM concentration in suspension was 3.5 μg mL^{-1}.

146 | *Environ. Sci.: Nano*, 2015, **2**, 143–154

This journal is © The Royal Society of Chemistry 2015

Table 2 Difference of means between cleaned PM (cPM) and raw PM (rPM) for the different assays

| Nanomaterial	Difference of means ($|cPM| - |rPM|$)		
	0.1 wt%	1 wt%	10 wt%
	DCF (%)[a]		
Ag	−2.8	0.39	−4.6
NiO	0.31	−2.9	−4.1
TiO₂	−2.0	−0.09	−5.6
Ceria	−0.75	−0.14	−5.9[c]
C₆₀	−8.0[c]	−0.54	0.98
Fe₂O₃	−5.9[c]	−0.96	5.0[c]
CdSe QD	−4.7	−0.68	0.83
None (control)	2.7		
	AA (%)[b]		
Ag	−11[c]	−11[c]	−15[c]
NiO	−9.4	−7.5	−16
TiO₂	−15[c]	−6.5	−11
Ceria	−7.0	−6.4	−14
C₆₀	−8.5	−19[c]	−14
Fe₂O₃	−7.1	−11	−5.3
CdSe QD	−8.7	−14	−34[c]
None (control)	2.0		
	UA (%)[b]		
Ag	0.2	−0.2	0.4
NiO	−0.2	0.1	0.4
TiO₂	−0.4	−0.6	−0.4
Ceria	−1	−0.2	0.1
C₆₀	−1[c]	−0.4	0
Fe₂O₃	−0.7	−0.4	0.2
CdSe QD	−0.6	0.2	−0.4[c]
None (control)	0.2		
	GSH/GSSG		
Ag	13[c]	47[c]	1.2[c]
NiO	28[c]	83[c]	−3.0[c]
TiO₂	−1.4[c]	−21[c]	14[c]
Ceria	5.3[c]	79[c]	25[c]
C₆₀	4.6[c]	4.8[c]	10[c]
Fe₂O₃	16[c]	14[c]	0.51[c]
CdSe QD	20[c]	1.2[c]	−5.9[c]
None (control)	13[c]		
	DTT (%)[b]		
Ag	19[c]	14[c]	23[c]
NiO	18[c]	23[c]	36[c]
TiO₂	18[c]	28[c]	26[c]
Ceria	17[c]	27[c]	29[c]
C₆₀	14[c]	23[c]	20[c]
Fe2O3	16[c]	21[c]	21[c]
CdSe QD	19[c]	14[c]	23[c]
None (control)	15[c]		

Positive values for dichlorofluorescein (DCF), ascorbic acid (AA), uric acid (UA), and dithiothreitol (DTT) indicate that cPM had higher OP than rPM. Negative values for reduced glutathione/oxidized glutathione (GSH/GSSG) indicate that cPM had higher OP than rPM. [a] % change in fluorescent intensity. [b] % antioxidant consumed. [c] Indicates significant difference between rPM and cPM at $p < 0.05$.

Cytotoxicity and genotoxicity response

We used the WST-1 assay to measure the cytotoxicity of PM. Viable cells cleave the WST-1 reagent to highly colored formazan because they have higher mitochondrial dehydrogenase activity than do non-viable cells. Differences in the viability of rPM and cPM compared to their corresponding
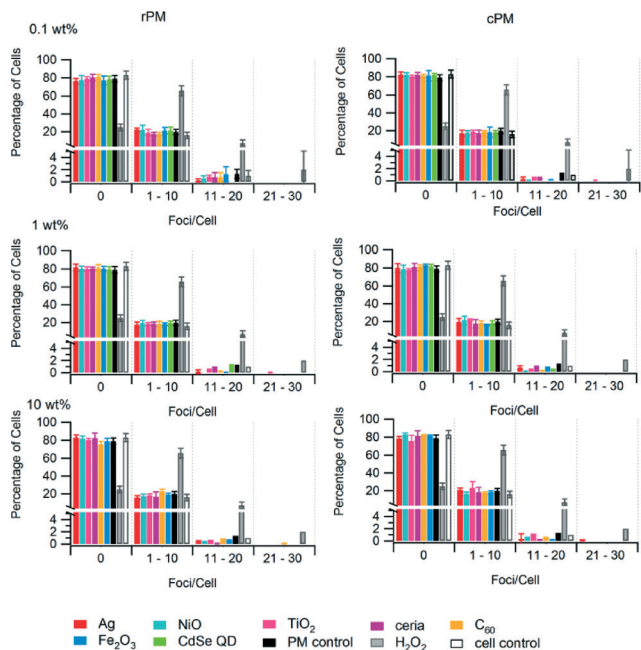
control at all incubation times were not significant (Fig. 6). For the types of nanomaterials and loadings considered in this study, the PM generated by incineration did not result in any significant decrease in the viability of the cells compared to the control. Even at longer incubation times up to 4 h, there were no significant differences. For most samples, there was no significant difference between rPM and cPM except for those containing 0.1 wt% ceria, 1 and 10 wt% TiO₂, and between rPM and cPM controls.

The phospho-histone H2AX (γH2AX) immunofluorescence assay considers the phosphorylation of H2AX as an endpoint of genotoxicity, and the number of foci correlates with an increase in DNA double strand breaks (DSB). Of the 200 cells we counted, ~20% exhibited 1–10 foci per cell, and less than 2% exhibited 11–20 foci per cell (Fig. 7). Cells without foci accounted for 78% to 86% of the 200. We did not observe cells containing more than 20 foci with the exception of the positive control (H₂O₂). The number of foci per cell was similar across different nanomaterials and was not significantly different compared to the control for rPM and cPM. There was no trend in the type or loading of the nanomaterials that induced the most foci, although samples containing Ag, TiO₂, ceria, and Fe₂O₃ formed more than 11 and up to 30 foci per cell for less than 2% of the cells. Only cPM from 0.1 wt% C₆₀ formed >30 foci per cell for 0.5% of the cells counted (data not shown). Although the values presented in Fig. 7 were corrected for the number of foci present in the control cells, cell-to-cell variation in the background γH2AX signal arising during DNA replication primarily in the S and G₂/M phases of the cell cycle[47,48] may have contributed to the foci we
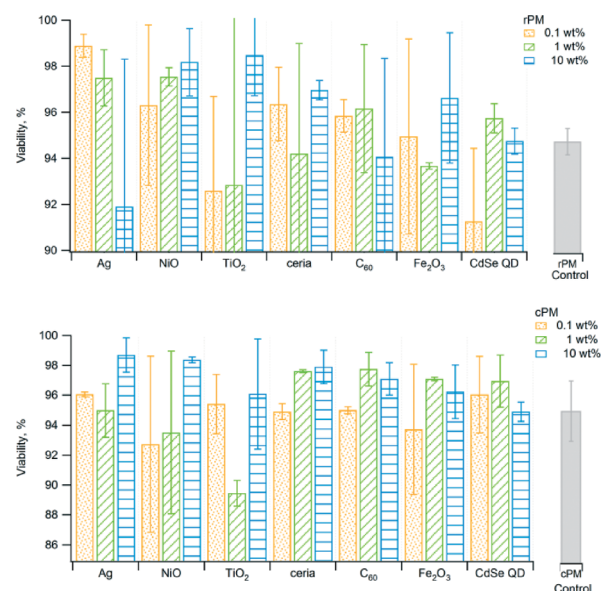
Fig. 6 Viability of A549 cells in the WST-1 assay after 2 h of exposure to raw PM (rPM) and cleaned PM (cPM) emitted from incineration of waste containing different nanomaterials at three mass loadings. Error bars represent standard deviations of three independent experiments. All samples except the positive control (H₂O₂) were not significantly different from the corresponding unspiked rPM or cPM control ($p > 0.05$). The PM concentration in suspension was 20 μg mL⁻¹.

This journal is © The Royal Society of Chemistry 2015

Environ. Sci.: Nano, 2015, 2, 143–154 | 147

Fig. 7 Formation of γH2AX foci in A549 cells after treatment of raw PM (rPM) and cleaned PM (cPM) emitted from nanowaste incineration containing different nanomaterials and mass loadings. Error bars represent standard deviations of three independent experiments. Columns lacking error bars have relative standard deviations of <5%. All samples except the positive control (H_2O_2) were not significantly different from the corresponding unspiked rPM or cPM control ($p > 0.05$). The PM concentration in suspension was 20 μg mL^{-1}.

counted. We have divided the category x-axes of Fig. 7 into four bins: no foci, 1–10 foci per cell, 11–20 foci per cell, and 21–30 foci per cell. Counting the number of foci per cell better distinguishes the extent of genotoxic response of A549 cells from the background γH2AX contribution.

Discussion

Little is known about the extent to which the interaction of nanomaterials and waste during combustion might modify the toxicity of the PM that is generated.[49,50] Nanomaterials themselves in the PM might be toxic, or they could enhance or mitigate toxic effects of other components of the PM. Results of our study suggest that the addition of nanomaterials to the incineration waste stream does not significantly affect the OP, cytotoxicity, or genotoxicity of PM in the fly ash under conditions tested, except for elevated ROS response in the GSH and DTT assays with Ag, TiO$_2$, and C$_{60}$. However, there are a number of caveats that should be considered.

Limitations

Only a small amount (0.023–180 mg g^{-1}) of nanomaterials partitioned into the PM versus the bottom ash.[45] For most nanomaterials, their mass fractions in PM were no more than 0.62% at any loading in the waste. The one exception was C$_{60}$, with mass fractions in the PM up to 26%. Thus, the subsequent discussion hinges on the fact that the amount of

nanomaterials in samples subjected to ROS and toxicity assays was very low in most cases, but it is possible that they catalyzed formation or destruction of other toxic compounds in the PM.

Results of the ROS assays must be interpreted with caution because of potential interference of PM with the assays. Initially, we performed the experiment at a PM concentration in suspension relevant to human exposure, ~20 μg mL^{-1} calculated for a 24 h exposure for a child at rest assuming that 65% of PM at a concentration of 35 μg m^{-3} (24 h National Ambient Air Quality Standard for PM$_{2.5}$) is deposited in the lungs[51] and that the mucus and alveolar fluid volume is 12.6 mL.[52,53] However, at this PM concentration, the fluorescence intensity of DCF, which should have increased, actually decreased, possibly because of the high surface area of PM that adsorbed the DCF and the enzyme. Thus, we used a lower concentration (3.5 μg mL^{-1}) of PM based on recommendations from studies of carbon black, which has similar optical properties to those of our PM.[54] At this concentration, we estimate the amount of the antioxidants that could adsorb to the particle surface to be <~0.2% for TiO$_2$, which has the highest specific surface area among the nanomaterials, assuming perpendicular adsorption geometry.

Another concern is the stability of the antioxidants, and, thus, the incubation time. Autooxidation, especially for ascorbic acid, dithiothreitol, and glutathione becomes dominant at incubation times longer than 1 h.[55] Therefore, we decided to simply measure antioxidant loss after 1 h, instead of measuring the consumption rate. We did not use shorter incubation times than 1 h because then there would be no significant losses for most of the antioxidants.[51]

The loss of antioxidants may be due to oxidative loss (both from ROS and non-ROS such as oxygen), adsorption onto particles, or both. Since the calculated amount of antioxidants adsorbing onto particles is small compared to the measured depletion, oxidative loss by ROS is presumed to be the dominant mechanism. This is supported by the appearance of GSSG from oxidation of GSH by ROS. Oxidation of GSH by oxygen over 1 h is a less likely explanation as it requires pH greater than 8.5 and copper salt as a catalyst.[56]

As with any acellular and in vitro assays, this study does not accurately reflect OP in vivo, and ROS formation can be underestimated or overestimated in some instances. We used particles in a physiological buffer that lacks the complexity of a biological system. Proteins, lipids, and other biological components can cause particles to aggregate and alter the toxicity of PM. In biological systems, the superoxide anion radical can liberate Fe^{2+} bound in Fe–S cluster proteins and amplify the formation of hydroxyl radicals.[57] Also, relatively inert species with no OP in vitro can become active in vivo, and soluble metals in aqueous/biological media can increase ROS production. In addition, since the biological defense system is protected by an array of antioxidants, OP might have been overestimated when measured using a single antioxidant, as the compounded effects of the antioxidants were not considered. Despite these

148 | Environ. Sci.: Nano, 2015, 2, 143–154

This journal is © The Royal Society of Chemistry 2015

limitations, this work still offers valuable information since the relative trend of ROS formation for the various nano-materials could still be valid in cellular system.

To address some of the limitations of the acellular assays, we assessed the cytotoxicity and genotoxicity response of A549 human lung epithelial cells to PM using the WST-1 and the γH2AX assays, respectively. At the tested concentration of nanomaterials, either as pure nanomaterials or as nano-materials that partitioned into the PM of incinerated waste, no cytotoxicity or genotoxicity was evident. This may be due to the small amount of nanomaterials that partitioned into the PM,[45] although other work has shown that even at higher concentrations, silver nanoparticles deposited at the air–liquid interface cause negligible cytotoxicity and only a mild inflammatory response to A549 cells.[58] However, Ag, TiO$_2$, and C$_{60}$ are of concern because they can catalyze the formation of high amounts of furans[9] or perhaps other pol-lutants that are more genotoxic. Another consideration is that cumulative toxicity over time is more likely to occur under natural settings than those imposed by experimental condi-tions. Other factors may also explain the negative results. Nanomaterials that generate ROS through a Fenton-like reac-tion depend on the interaction between the surface of PM and the bulk media. Metal nanomaterials may act as con-densation nuclei for organic species, and they may not be available for reactions if they are buried underneath layers of organic species. Although our results suggest that some nanomaterials in consumer products that are incinerated[45] will not modify the toxicity of the PM in the exhaust, these results should be interpreted with caution.

Particle size

Although particle size and surface area are critical factors in determining the toxicity of PM,[59] our results suggest that they were not the dominant determinants of toxicity under the conditions examined in this study. rPM and cPM that were similar in size exhibited significantly different toxicity in the GSH/GSSG and DTT assays.

Organics

ROS can be generated by ROS-active adsorbed organic com-ponents or through conversion of labile components to ROS-active species. In the ascorbic acid assay, rPM displayed higher OP than did cPM in some cases, suggesting that some adsorbed organic species actively oxidize ascorbic acid or generate species that oxidize it. PAHs are abundant in combustion-generated PM. They are ROS-inactive in vitro, although the presence of ascorbic acid[60] or other reductants and superoxide anion radicals might convert some of the PAHs and organic species to ROS-active quinonic species.[46,61,62] Our study on combustion by-product emissions[9] shows that Ag and TiO$_2$ catalyze the formation of furans. While the toxicity of furans is not attributed to ROS formation, the highly electrocatalytic nature of Ag may perhaps also catalyze the formation of other species that are unmonitored but are ROS-active, such as environmentally persistent free

radicals.[63] These species may be responsible for the elevated antioxidant consumption (glutathione and ascorbic acid) of rPM relative to cPM containing Ag (Table 2).

Among the nanomaterials considered in this study, C$_{60}$ persists best through the combustion zone.[45] The higher fluorescence intensity for rPM compared to cPM containing 0.1 wt% C$_{60}$ suggests that adsorbed organic species are dominant in catalyzing ROS formation. The majority of the literature reports little or no toxicity for C$_{60}$ in vitro, but it has been shown to generate ROS in vivo[64,65] when irradi-ated. Since this work took place under non-irradiated condi-tions, the increase in consumption of antioxidants is pri-marily attributed to the adsorbed organic species and metals rather than C$_{60}$. This hypothesis is supported further by 1) the similar OP between rPM and cPM from 10 wt% C$_{60}$ waste despite the elevated amount of C$_{60}$ in rPM (i.e., the cleaning procedure removed some C$_{60}$), 2) the simi-lar level of ascorbic acid consumption for rPM and cPM compared to the control, and 3) the lower OP of pure C$_{60}$ nanoparticles in most assays. Indeed, carbon black, which contains organic species and metals, has been reported to promote greater ROS formation than fullerenes because of adsorbed organic components.[65]

Metals

Aside from organics, metals in certain oxidation states can also generate ROS.[66] Redox-active metals can donate electrons to forming superoxide anion radicals that can then dismutate, forming hydrogen peroxide. Hydrogen peroxide can then react with metals and form hydroxyl radicals. The elevated magnitude of antioxidant consumption for cPM compared to rPM in some assays, especially ascorbic acid for Ag, GSH/GSSG for TiO$_2$ at 1 wt%, and DTT for all nano-materials, suggests that the extraction of organic species from PM exposes the catalytic surface of metals, resulting in higher OP. As shown in Table S1,† PM from the control waste contained substantial amounts of metals, which originated from the paper, polyethylene, and poly(vinyl chloride). Although most metals in PM, such as exogenous iron, exist mainly in their higher oxidation states[67] and are immobilized in the particle,[68] and therefore are ROS-inactive, reductants can convert them to a form that is ROS-active. Whereas metals in PM are usually present in higher oxidation states, and thus are ROS-inactive, metals in nanomaterials that are incinerated with the waste are in a different form (e.g., crystalline phase) and could potentially generate ROS. For most nanomaterials, OP is one of the primary mecha-nisms of toxicity.[69] The combination of ROS formation[70–72] by the nanoparticles and release of the core metal (Cd)[72] may be responsible for the higher OP for 10 wt% CdSe QD rPM.

Differences between ROS assays

It appears that the different antioxidants have varying sensi-tivity towards a specific class of chemical species in PM. For instance, adsorbed organic species are more sensitive

This journal is © The Royal Society of Chemistry 2015

Environ. Sci.: Nano, 2015, 2, 143–154 | 149

towards glutathione and ascorbic acid, while metals are most sensitive towards DTT. Therefore, a battery of assays should be used to assess and to establish the toxicity of PM, and results of acellular assays should be validated with cell-based assays. Most results in the literature have suggested that the DTT assay is insensitive to metals as it only measures the superoxide anion radical. However, the higher activity for cPM, which likely has more exposed metals, in the present work agrees with other studies that also observed higher DTT activity for some transition metals compared to organic components.[73–75] The higher DTT consumption of cPM cannot be attributed to redox-cycling organic species, as they were mostly removed. Also, the DTT assay may be sensitive to the form of metals, whether they are bound on the surface of the particles or soluble.[76]

The GSH/GSSG and DTT assays may be sensitive to different species in the PM, as they indicated a difference in OP between rPM and cPM (Table 2). rPM exhibited stronger OP in the GSH/GSSG assay but lesser OP in the DTT assay compared to cPM. We hypothesize that in a biological system, initially organic species are responsible for ROS generation. However, as the shell of organic species is exfoliated from the particle over time, the metal-containing core of the PM becomes exposed, amplifying ROS generation. The results suggest that the OP of the PM more strongly depends on the adsorbed organic or inorganic components than the presence of the nanomaterials, at least at the very low levels seen in this study.

Previous nanomaterial and aerosol characterization. In our previous study,[45] we characterized PM generated by incineration of waste dosed with 0.1 wt% and 10 wt% nanomaterials. At a loading of 0.1 wt%, the median size of the PM was ~390 nm, similar in size to PM produced from the control waste that did not contain any nanomaterials. At a loading of 10 wt%, the median size of the PM was significantly smaller, ~325 nm. TEM analysis of PM that was collected on a filter and suspended in methanol revealed formation of fractal aggregates of carbonaceous PM, and there were no apparent differences in size and morphology by type of nanomaterial, including the control (Fig. S1†).

The majority of nanomaterials partitioned into the bottom ash and retained their original size and morphology, although they formed large aggregates. We observed phase transition of anatase-TiO_2 to rutile-TiO_2 in the bottom ash. The phase transition of TiO_2,[77] the formation of Ag–O and chemisorbed oxygen may have contributed to an increase in OP. We were not able to find any nanomaterials in the PM to subject them to elemental and diffraction analysis, but we hypothesize that they may have undergone similar changes compared to nanomaterials in the bottom ash. It is also possible that they may have been modified further as they reacted with numerous combustion by-products upon entering and exiting different combustion zones. For most samples, the absence of a significant difference in toxicity from the control hinges on the fact that only a small amount of nanomaterials partitioned into the PM. The mass of

Table 3 Mass of nanomaterials contained in PM used for cell-based assays

Nanomaterial	Mass[a] (ng)		
	0.1 wt%[b]	1 wt%[b]	10 wt%[b]
Ag	1.99	2.07	3.72
NiO	7.06	c	c
TiO_2	0.298	0.125	0.228
Ceria	nd[d]	nd[d]	0.217
C_{60}[e]	nd[d]	362	526
Fe_2O_3	c	c	c
CdSe QD[f]	1.00	4.86	0.480

[a] All values are corrected for the metal/metal oxide/C_{60} concentration in the unspiked control waste. The relative standard deviation for six of the samples (two samples at each mass loading) that were run in duplicate was less than 12%. [b] Original nanomaterial loading in waste that was subject to incineration. [c] Amount was higher in PM from unspiked control waste. [d] Not detected. [e] Measured by HPLC. [f] Measured as Cd.

nanomaterials that partitioned into the PM that was used in the toxicity assays ranged from 0.125 to 7.06 ng, except for C_{60}, which resulted in several hundreds of nanograms in the PM (Table 3). Furthermore, only one-sixth of this amount was used in the acellular assays.

Conclusions

Incineration as end-of-life treatment for nanowaste has perhaps the greatest potential among disposal methods for transforming nanomaterials and affecting emissions to the environment, particularly those of PM as a combustion by-product. In this study, the presence of certain nanomaterials did not affect the OP, cytotoxicity, and genotoxicity of PM generated by incineration under the conditions investigated. However, PM emitted from incineration of waste containing three of the nanomaterials (Ag, TiO_2, and C_{60}) exhibited elevated OP, while four of the nanomaterials (NiO, ceria, Fe_2O_3, and CdSe QD) did not. These results suggest an urgent need to study the toxic effects of these nanomaterials in more detail, as they are currently produced and used in relatively large quantities.

One limitation of the current experimental protocol is the small dose of PM; there may be significant differences in the toxicity of the particles at higher doses. This study relies heavily on chemical markers, whose sensitivity to different components of PM varies. To complement the results from this study, we suggest future research focusing on a marker such as gene expression and assessing OP in cellular systems, using a battery of cellular-based assays, as the present study included only two assays. Additionally, the interaction among the nanomaterials, organic pollutants, and chemical markers may be diffusion-limited, and observation of any significant toxic effects may require longer exposure times. A more complete assessment of the toxicity of PM generated from nanowaste incineration will include in vivo and in vitro studies with both subchronic and chronic exposures, as some toxic

effects only appear when a significant amount of a toxicant has accumulated in the organism.

Experimental

Nanomaterials

Seven nanomaterials were investigated: silver (Ag, coated with poly(vinyl pyrrolidone), NanoAmor, 30–50 nm, 5–10 m^2 g^{-1}, ≥99.5%), nickel oxide (NiO, NanoAmor, 10–20 nm, 50–80 m^2 g^{-1}, ≥99.8%), titania (TiO_2, particle size <25 nm, specific surface area 200–220 m^2 g^{-1}, purity ≥99.7%), ceria (NanoAmor, 15–30 nm, 30–50 m^2 g^{-1}, ≥99.9%), C_{60}-fullerene (C_{60}, SES Research, ≥99.8%), iron oxide (Fe_2O_3, <30 nm, ≥99%), and CdSe/ZnS quantum dots (CdSe QD). The nanoparticles were dispersed in ethanol, with the exception of C_{60} which was dissolved in toluene. All chemicals were purchased from Sigma-Aldrich unless otherwise noted.

Particle collection and clean-up

Waste containing a mixture of equal amounts of paper, polyethylene, and poly(vinyl chloride) spiked with nanomaterials was incinerated at 850 °C with 1 L min^{-1} of clean and particle-free air. The resulting PM was collected onto a polytetrafluoroethylene (PTFE) filter (diameter 47 mm, pore size 0.1 μm) as described elsewhere.[9] In the interest of trying to separate the effects of adsorbed organic species from effects stemming from the core of the PM, extracts of both raw PM (rPM) and cleaned PM (cPM) were prepared. PM was cleaned by extracting the adsorbed organic species in a series of solvents by sonicating for 15 min, centrifuging at 20 000g for 10 min, and removing the supernatant. Extraction was repeated with 1 mL cyclohexane, then 1 mL acetone, then three times with 1 mL of cyclohexane : acetone solution (1 : 1, v/v), and finally with 1 mL dichloromethane. Residual solvent was removed by air-drying for 12 h at ambient temperature and pressure. The following samples were tested: rPM, cPM, pure nanomaterial in suspension, PM produced from unspiked wastes, and H_2O_2 as a positive control. The final particle suspensions were resuspended in ethanol and stored at −20 °C. The particle suspensions were sonicated in a bath sonicator three times for 5 s just prior to use in the assays to minimize formation of free radicals from the homolytic cleavage of water.

Dichlorofluorescein (DCF) assay

The DCF assay[78] is a widely used acellular measure of ROS. Briefly, 0.5 mL of 2′,7′-dichlorodihydrofluorescein diacetate (H_2-DCFHDA) was hydrolyzed with 2 mL of 0.01 N NaOH to 2′,7′-dichlorodihydrofluorescin, incubated in the dark for 30 min, and then neutralized with 25 mL of 100 mM, pH 7.4 phosphate-buffered saline (PBS). Twenty two milliliters of horse radish peroxidase (HRP) solution in PBS, containing 4.95 units mL^{-1} was then added to the H_2-DCFHDA. A 20 μL suspension of particles prepared as described above was added to 1 mL of the prepared reaction mixture in an

amber microcentrifuge tube. The final particle concentration was 3.5 μg mL^{-1}. The suspension was incubated in an orbital mixer at 37 ± 0.5 °C for 1 h. After incubation, the suspension was equilibrated in a water bath at 25 °C for 5 min, centrifuged at 20 000g for 10 min, and filtered through a nylon membrane filter (diameter 4 mm, pore size 0.2 μm). A 200 μL aliquot was plated into a 96-well microtiter plate. Formation of DCF was monitored as an increase in fluorescence intensity at 490 nm excitation and 520 nm emission wavelengths with a multiplate fluorescence reader (SpectraMax M2[e], Molecular Devices). Ethanol was used as a blank and 10 μM H_2O_2 as a positive control. ROS formation was quantified as the relative percentage of fluorescence less the blank. Since a high concentration of PM interferes with the DCF assay,[54] we supplemented the measurement of OP with measurement of the depletion of antioxidants, described below.

Ascorbic (AA) and uric acid (UA) assays

A 20 μL suspension of PM (180 μg mL^{-1}) was added to 1 mL of 20 μM ascorbic acid solution in PBS, vortexed, and incubated at 37 ± 0.5 °C for 1 h in the dark on a shaker. After incubation, the samples were equilibrated to 25 °C for 5 min, augmented with 500 μL of 100 μM of dithiothreitol (DTT) to prevent auto-oxidation, filtered through a nylon membrane filter (diameter 4 mm, pore size 0.2 μm), and refrigerated at −80 °C prior to analysis. All analyses were completed within 24 h after incubation with the antioxidants. Samples for the uric acid assay were prepared in a similar manner, except no DTT was added. The uric acid solution (20 μM) was prepared by dissolving uric acid in 1 mL of 0.01 N NaOH, diluting with PBS, and then neutralizing with an equimolar amount of HCl. Ethanol was used a blank and 10 μM H_2O_2 as a positive control. Values were reported as relative percentage of antioxidant consumed less the blank.

Analysis was performed isocratically with a high-performance liquid chromatograph (HPLC, LC-MS 2020, Shimadzu Inc.) equipped with an ultraviolet absorption detector. Sample volumes of 10 μL were eluted with a 0.1 M KH_2PO_4–H_3PO4 (pH 2.1) mobile phase through a 25 cm reverse-phase column. Samples were refrigerated at 15 °C during the analysis. Calibration standards were run with each set of samples, and a linear response was confirmed with three of the calibration standards after injection of 12 samples. The ascorbic acid and uric acid signals were monitored at 254 nm and 280 nm, respectively. Ascorbic acid analysis was performed within 3 h to minimize the opportunity for auto-oxidation.

Glutathione (GSH) assay

Consumption of glutathione was measured by the enzymatic recycling assay as described elsewhere.[79] Briefly, 1 mL of 50 μM of reduced glutathione solution in PBS was added to a 20 μL of suspension of particles and treated as described above. After incubation, 50 μL aliquots of the samples were plated in a 96-well microtiter plate, and 150 μL of the reaction mixture containing 30 μM 5,5′-dithio-bis(2-nitrobenzoic acid)

This journal is © The Royal Society of Chemistry 2015

Environ. Sci.: Nano, 2015, 2, 143–154 | 151

(DTNB) and 0.171 unit mL^{-1} glutathione reductase (a gift from Bio-Research Products, Inc.) in 100 mM PBS (pH 7.4) containing 20 μM ethylenediaminetetraacetic acid (EDTA) (referred hereafter as PBS-EDTA) was added. The samples were incubated for 5 min at ambient temperature, and 50 μL of 38 μM reduced nicotinamide adenine dinucleotide phosphate (NADPH) solution in PBS-EDTA was added to initiate the reaction. After 25 min, the absorbance was read at 405 nm with a multiplate reader (μQuant, BioTek) to measure the total glutathione. Since no other thiol-containing compound other than glutathione was present, for the exclusive measurement of reduced glutathione, glutathione reductase in the reaction mixture was replaced with PBS-EDTA. The amount of oxidized glutathione was determined from the total glutathione (oxidized and reduced glutathione) less the reduced glutathione.

Dithiothreitol assay

The DTT assay followed a previously described procedure.[73] Briefly, 1 mL of 50 μM DTT solution in PBS was added to 20 μL of sample. The suspension was treated as described above. After incubation, the reaction was quenched with 500 μL of 10% (v/v) trichloroacetic acid, which also prevented further DTT oxidation. Sample aliquots of 100 μL were plated in a 96-well microtiter plate, and 150 μL of 30 μM DTNB in Tris–HCl (pH 8.9) buffer was added. The mixture was agitated, incubated for 10 min, and the absorbance was read at 405 nm with a multi-plate reader (μQuant, BioTek).

Cell culture

A549 human alveolar lung epithelial cells (ATCC, #CCL-185, Manassas, VA) were routinely subcultured in Dulbecco's Modified Eagle Medium (DMEM, Thermo Scientific HyClone, Logan, UT) supplemented with heat-inactivated 10% fetal bovine serum (FBS) and 1% penicillin–streptomycin (Thermo Scientific HyClone, Logan, UT). The cells were maintained in a humidified incubator at 37 °C and 5% CO$_2$.

WST-1 cytotoxicity test

A 96-well polystyrene plate was seeded with 2×10^4 cells per well in 100 μL media. After 12 h, once the cells adhered, they were treated with 37 μL of sample containing 20 μg mL^{-1} of the PM suspension. The suspensions were prepared by dispersing PM and cPM in 0.1% (v/v) Tween-20 in PBS solution (pH 7.4). After treatment, the cells were incubated at 37 °C for 24 h, and then 13.7 μL of the WST-1 reagent (Roche, Indianapolis, IN) was added to each sample. The absorbance was read after 2, 3, and 4 h of incubation (Tecan Safire^2 Microplate Reader, Tecan US Inc., Research Triangle Pa, NC) at 440 nm with a reference wavelength of 660 nm. Samples were run three times with three replicates for each run. At the PM concentration used, there was no significant difference in absorbance between the sample containing PM in the cell media and the sample that contained only the cell media and no PM.

Phospho-histone H2AX (γH2AX) immunofluorescence assay for genotoxicity

A 96-well polystyrene plate was seeded with 1×10^4 cells per well. The cells were then treated with 37 μL of sample containing 20 μg mL^{-1} of the PM suspension and incubated for 24 h. Cells were then fixed with 4% paraformaldehyde for 15 min and permeabilized in 0.25% Triton X-100 for 15 min. Bovine serum albumin in PBS at 1% (v/v) was used as blocking serum for 1 h, and cells were incubated with a rabbit polyclonal anti-γH2AX antibody (1 : 500, Santa Cruz Biotechnology Inc.) for 1 h at room temperature. The wells were washed three times with PBS, and were incubated with Alexa Fluor 488 Goat Anti-Rabbit IgG (H + L) Antibody (1 : 500, Life Technologies Corporation) and Hoechst 33342 (10 μg mL^{-1}, Life Technologies Corp.) for 1 h. The cells were washed three times with PBS and visualized under a fluorescent microscope equipped with FITC and DAPI filters (Olympus). Cells without treatment and those treated with 100 μM H$_2$O$_2$ were incubated for 10 min at 37 °C to serve as negative and positive controls, respectively. Images were acquired using a 40× objective with a fluorescent microscope (EcLipse TS 100, Nikon, Melville, NY). Images for 200 cells were analyzed using ImageJ 1.47 with a macro designed to subtract the response of the background and to count the number of foci within a defined nuclear mask.

Hydrodynamic size measurement

The hydrodynamic size of PM suspensions in PBS with 0.1 wt% Tween-20 was measured by dynamic light scattering (DLS, Malvern Zetasizer Nano). PM suspensions at a concentration of 35 μg mL^{-1} were sonicated for 30 s prior to measurement. A more detailed characterization of the PM exhaust other than the hydrodynamic size is presented in our previous study.[45]

Analysis of PM by Transmission Electron Microscopy (TEM)

PM on filters was suspended in acetone-free methanol. The suspension was sonicated for 2 min, diluted 100×, and then sonicated again, prior to drop-casting 10 μL of the suspension onto a 200 mesh, lacey-carbon-coated copper TEM grid. The samples were stored under vacuum or nitrogen until analysis. A Philips EM420 TEM (Philips Corporation) operated at 120 kV was used to acquire images.

Statistical analysis

Differences in the data set were analyzed with one-way ANOVA with Dunnet's post-hoc test at $p < 0.05$ for comparison with PM from the control using the Igor Pro™ statistical package. Differences between PM and cPM were compared using a two-tailed Student's t-test at $p < 0.05$.

Acknowledgements

152 | Environ. Sci.: Nano, 2015, 2, 143–154

This journal is © The Royal Society of Chemistry 2015

Notes and references

1 F. Cangialosi, G. Intini, L. Liberti, M. Notarnicola and P. Stellacci, *Waste Manage.*, 2008, **28**, 885–895.

2 V. E. Archer, *Arch. Environ. Health*, 1990, **45**, 325–334.

3 M. Bobak and D. A. Leon, *Lancet*, 1992, **340**, 1010–1014.

4 J. S. Evans, T. Tosteson and P. L. Kinney, *Environ. Int.*, 1984, **10**, 55–83.

5 L. B. Lave and E. P. Seskin, *Science*, 1970, **169**, 723–733.

6 F. W. Lipfert, *J. Environ. Econ. Manage.*, 1984, **11**, 208–243.

7 H. Özkaynak and G. D. Thurston, *Risk Anal.*, 1987, **7**, 449–461.

8 C. A. Pope 3rd, M. J. Thun, M. M. Namboodiri, D. W. Dockery, J. S. Evans, F. E. Speizer and C. W. Heath Jr., *Am. J. Respir. Crit. Care Med.*, 1995, **151**, 669–674.

9 E. P. Vejerano, A. L. Holder and L. C. Marr, *Environ. Sci. Technol.*, 2013, **47**, 4866–4874.

10 T. Walser, L. K. Limbach, R. Brogioli, E. Erismann, L. Flamigni, B. Hattendorf, M. Juchli, F. Krumeich, C. Ludwig, K. Prikopsky, M. Rossier, D. Saner, A. Sigg, S. Hellweg, D. Gunther and W. J. Stark, *Nat. Nanotechnol.*, 2012, 7, 520–524.

11 J. Y. Han, K. Takeshita and H. Utsumi, *Free Radical Biol. Med.*, 2001, **30**, 516–525.

12 A. K. Prahalad, J. Inmon, L. A. Dailey, M. C. Madden, A. J. Ghio and J. E. Gallagher, *Chem. Res. Toxicol.*, 2001, **14**, 879–887.

13 A. K. Prahalad, J. M. Soukup, J. Inmon, R. Willis, A. J. Ghio, S. Becker and J. E. Gallagher, *Toxicol. Appl. Pharmacol.*, 1999, **158**, 81–91.

14 A. M. Knaapen, T. M. Shi, P. J. A. Borm and R. P. F. Schins, *Mol. Cell. Biochem.*, 2002, **234**, 317–326.

15 A. P. Breen and J. A. Murphy, *Free Radical Biol. Med.*, 1995, **18**, 1033–1077.

16 G. Cohen, S. Yakushin and D. Dembiec-Cohen, *Anal. Biochem.*, 1998, **263**, 232–239.

17 H. W. Gardner, *Free Radical Biol. Med.*, 1989, **7**, 65–86.

18 A. W. Girotti, *Free Radical Biol. Med.*, 1985, **1**, 87–95.

19 S. A. Gurgueira, J. Lawrence, B. Coull, G. G. K. Murthy and B. Gonzalez-Flecha, *Environ. Health Perspect.*, 2002, **110**, 749–755.

20 K. Hirakawa, S. Oikawa, Y. Hiraku, I. Hirosawa and S. Kawanishi, *Chem. Res. Toxicol.*, 2002, **15**, 76–82.

21 G. Oberdorster, R. M. Celein, J. Ferin and B. Weiss, *Inhalation Toxicol.*, 1995, **7**, 111–124.

22 G. Oberdorster, J. Ferin, J. Finkelstein and S. Soderholm, *Acta Astronaut.*, 1992, **27**, 251–256.

23 G. Oberdorster, J. Ferin, S. Soderholm, R. Gelein, C. Cox, R. Baggs and P. E. Morrow, *Ann. Occup. Hyg.*, 1994, **38**, 295–302.

24 A. Peters, D. W. Dockery, J. E. Muller and M. A. Mittleman, *Circulation*, 2001, **103**, 2810–2815.

25 W. A. Pryor, K. Stone, L. Y. Zang and E. Bermudez, *Chem. Res. Toxicol.*, 1998, **11**, 441–448.

26 G. L. Squadrito, R. Cueto, B. Dellinger and W. A. Pryor, *Free Radical Biol. Med.*, 2001, **31**, 1132–1138.

27 A. Valavanidis, A. Salika and A. Theodoropoulou, *Atmos. Environ.*, 2000, **34**, 2379–2386.

28 T. S. Hiura, N. Li, R. Kaplan, M. Horwitz, J.-C. Seagrave and A. E. Nel, *J. Immunol.*, 2000, **165**, 2703–2711.

29 N. Li, C. Sioutas, A. Cho, D. Schmitz, C. Misra, J. Sempf, M. Wang, T. Oberley, J. Froines and A. Nel, *Environ. Health Perspect.*, 2003, **111**, 455–460.

30 T. Xia, P. Korge, J. N. Weiss, N. Li, M. I. Venkatesen, C. Sioutas and A. Nel, *Environ. Health Perspect.*, 2004, **112**, 1347–1358.

31 B. Wang, J.-J. Yin, X. Zhou, I. Kurash, Z. Chai, Y. Zhao and W. Feng, *J. Phys. Chem. C*, 2012, **117**, 383–392.

32 M. I. Khan, A. Mohammad, G. Patil, S. A. H. Naqvi, L. K. S. Chauhan and I. Ahmad, *Biomaterials*, 2012, **33**, 1477–1488.

33 Y. Pan, A. Leifert, D. Ruau, S. Neuss, J. Bornemann, G. Schmid, W. Brandau, U. Simon and W. Jahnen-Dechent, *Small*, 2009, **5**, 2067–2076.

34 Y. Yamakoshi, N. Umezawa, A. Ryu, K. Arakane, N. Miyata, Y. Goda, T. Masumizu and T. Nagano, *J. Am. Chem. Soc.*, 2003, **125**, 12803–12809.

35 M. Bottini, S. Bruckner, K. Nika, N. Bottini, S. Bellucci, A. Magrini, A. Bergamaschi and T. Mustelin, *Toxicol. Lett.*, 2006, **160**, 121–126.

36 C. M. Goodman, C. D. McCusker, T. Yilmaz and V. M. Rotello, *Bioconjugate Chem.*, 2004, **15**, 897–900.

37 A. Gliga, S. Skoglund, I. Odnevall Wallinder, B. Fadeel and H. Karlsson, *Part. Fibre Toxicol.*, 2014, **11**, 11.

38 L. M. Sargent, A. A. Shvedova, A. F. Hubbs, J. L. Salisbury, S. A. Benkovic, M. L. Kashon, D. T. Lowry, A. R. Murray, E. R. Kisin, S. Friend, K. T. McKinstry, L. Battelli and S. H. Reynolds, *Environ. Mol. Mutagen.*, 2009, **50**, 708–717.

39 S. Pfuhler, R. Elespuru, M. J. Aardema, S. H. Doak, E. Maria Donner, M. Honma, M. Kirsch-Volders, R. Landsiedel, M. Manjanatha, T. Singer and J. H. Kim, *Environ. Mol. Mutagen.*, 2013, **54**, 229–239.

40 S. Matsuda, S. Matsui, Y. Shimizu and T. Matsuda, *Environ. Sci. Technol.*, 2011, **45**, 4133–4138.

41 P. V. AshaRani, G. Low Kah Mun, M. P. Hande and S. Valiyaveettil, *ACS Nano*, 2008, **3**, 279–290.

42 Y. Kumagai, T. Arimoto, M. Shinyashiki, N. Shimojo, Y. Nakai, T. Yoshikawa and M. Sagai, *Free Radical Biol. Med.*, 1997, **22**, 479–487.

43 A. E. Nel, D. Diaz-Sanchez and N. Li, *Curr. Opin. Pulm. Med.*, 2001, **7**, 20–26.

44 P. H. N. Saldiva, R. W. Clarke, B. A. Coull, R. C. Stearns, J. Lawrence, G. G. K. Murthy, E. Diaz, P. Koutrakis, H. Suh, A. Tsuda and J. J. Godleski, *Am. J. Respir. Crit. Care Med.*, 2002, **165**, 1610–1617.

This journal is © The Royal Society of Chemistry 2015

Environ. Sci.: Nano, 2015, **2**, 143–154 | 153

45 E. P. Vejerano, E. C. Leon, A. L. Holder and L. C. Marr, *Environ. Sci.: Nano*, 2014, **1**, 133–143.

46 N. Li, T. Xia and A. E. Nel, *Free Radical Biol. Med.*, 2008, **44**, 1689–1699.

47 S. H. MacPhail, J. P. Banáth, Y. Yu, E. Chu and P. L. Olive, *Radiat. Res.*, 2003, **159**, 759–767.

48 X. Huang, T. Tanaka, A. Kurose, F. Traganos and Z. Darzynkiewicz, *Int. J. Oncol.*, 2006, **29**, 495–501.

49 M. C. Arnold, A. R. Badireddy, M. R. Wiesner, R. T. Di Giulio and J. N. Meyer, *Arch. Environ. Contam. Toxicol.*, 2013, 1–10.

50 M. Heinlaan, A. Ivask, I. Blinova, H.-C. Dubourguier and A. Kahru, *Chemosphere*, 2008, **71**, 1308–1316.

51 H. Zielinski, I. S. Mudway, K. A. Berube, S. Murphy, R. Richards and F. J. Kelly, *Am. J. Physiol.*, 1999, **277**, L719–L726.

52 G. E. Hatch, in *Comparative Biology of the Normal Lung*, ed. R. A. Parent, CRC, London, 1994, pp. 617–630.

53 M. B. Snipes, R. O. McClellan, J. L. Mauderly and R. K. Wolf, *Health Phys.*, 1989, **57**, 69–78.

54 A. Kroll, M. Pillukat, D. Hahn and J. Schnekenburger, *Arch. Toxicol.*, 2012, **86**, 1123–1136.

55 R. Kandar, P. Drabkova and R. Hampl, *J. Chromatogr., B*, 2011, **879**, 2834–2839.

56 M. B. Young and H. A. Young, *J. Am. Chem. Soc.*, 1942, **64**, 2282–2287.

57 M. A. Kohanski, D. J. Dwyer, B. Hayete, C. A. Lawrence and J. J. Collins, *Cell*, 2007, **130**, 797–810.

58 A. L. Holder and L. C. Marr, *BioMed Res. Int.*, 2013, **2013**, 1–11.

59 J. M. Hillegass, A. Shukla, S. A. Lathrop, M. B. MacPherson, N. K. Fukagawa and B. T. Mossman, *Wiley Interdiscip. Rev.: Nanomed. Nanobiotechnol.*, 2010, **2**, 219–231.

60 J. Verrax, M. Delvaux, N. Beghein, H. Taper, B. Gallez and P. B. Calderon, *Free Radical Res.*, 2005, **39**, 649–657.

61 A. Baulig, M. Sourdeval, M. Meyer, F. Marano and A. Baeza-Squiban, *Toxicol. In Vitro*, 2003, **17**, 567–573.

62 S. Lomnicki, H. Truong, E. Vejerano and B. Dellinger, *Environ. Sci. Technol.*, 2008, **42**, 4982–4988.

63 W. Gehling and B. Dellinger, *Environ. Sci. Technol.*, 2013, **47**, 8172–8178.

64 J. W. Arbogast, A. P. Darmanyan, C. S. Foote, F. N. Diederich, R. L. Whetten, Y. Rubin, M. M. Alvarez and S. J. Anz, *J. Phys. Chem.*, 1991, **95**, 11–12.

65 N. R. Jacobsen, G. Pojana, P. White, P. Møller, C. A. Cohn, K. Smith Korsholm, U. Vogel, A. Marcomini, S. Loft and H. Wallin, *Environ. Mol. Mutagen.*, 2008, **49**, 476–487.

66 D. Jassby, J. Farner Budarz and M. Wiesner, *Environ. Sci. Technol.*, 2012, **46**, 6934–6941.

67 U. E. A. Fittschen, F. Meirer, C. Streli, P. Wobrauschek, J. Thiele, G. Falkenberg and G. Pepponi, *Spectrochim. Acta, Part B*, 2008, **63**, 1489–1495.

68 U. Kukier, C. F. Ishak, M. E. Sumner and W. P. Miller, *Environ. Pollut.*, 2003, **123**, 255–266.

69 H. Meng, T. Xia, S. George and A. E. Nel, *ACS Nano*, 2009, **3**, 1620–1627.

70 N. Chen, Y. He, Y. Su, X. Li, Q. Huang, H. Wang, X. Zhang, R. Tai and C. Fan, *Biomaterials*, 2011, **33**, 1238–1244.

71 M. Green and E. Howman, *Chem. Commun.*, 2005, 121–123.

72 I. Pujalte, I. Passagne, B. Brouillaud, M. Treguer, E. Durand, C. Ohayon-Courtes and B. L'Azou, *Part. Fibre Toxicol.*, 2011, **8**, 10.

73 J. G. Charrier and C. Anastasio, *Atmos. Chem. Phys.*, 2012, **12**, 9321–9333.

74 P. Lin and J. Z. Yu, *Environ. Sci. Technol.*, 2011, **45**, 10362–10368.

75 A. Eiguren-Fernandez, M. Shinyashiki, D. A. Schmitz, E. DiStefano, W. Hinds, Y. Kumagai, A. K. Cho and J. R. Froines, *Environ. Res.*, 2010, **110**, 207–212.

76 A. K. Cho, C. Sioutas, A. H. Miguel, Y. Kumagai, D. A. Schmitz, M. Singh, A. Eiguren-Fernandez and J. R. Froines, *Environ. Res.*, 2005, **99**, 40–47.

77 K. Hirakawa, M. Mori, M. Yoshida, S. Oikawa and S. Kawanishi, *Free. Radical Res.*, 2004, **38**, 439–447.

78 R. Cathcart, E. Schwiers and B. N. Ames, *Anal. Biochem.*, 1983, **134**, 111–116.

79 M. A. Baker, G. J. Cerniglia and A. Zaman, *Anal. Biochem.*, 1990, **190**, 360–365.